Nanoscale

Accepted Manuscript

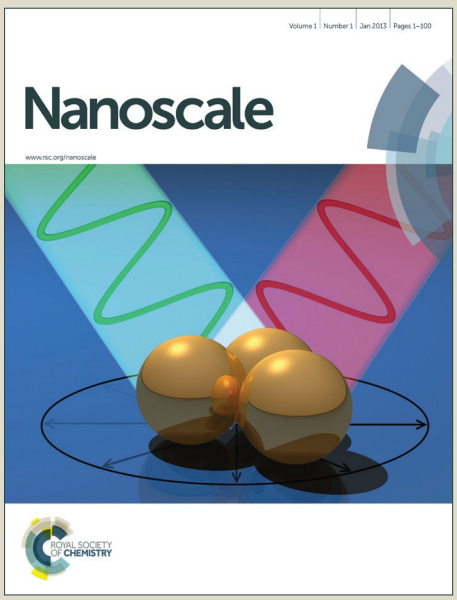

ROYAL SOCIETY OF CHEMISTRY

www.rsc.org/nanoscale

Journal Name

ARTICLE

Sensitizing basal-like breast cancer to chemotherapy using nanoparticles conjugated with interference peptide

Received 00th January 20xx,
Accepted 00th January 20xx

DOI: 10.1039/x0xx00000x

www.rsc.org/

A. Sorolla,[a] D. Ho,[b†] E. Wang,[a†] C. Evans,[b] C.F.G. Ormonde,[b] R. Rashwan,[a] R. Singh,[b] K. Swaminathan Iyer,[b*] and P.Blancafort[a*]

Basal-like breast cancers are highly aggressive malignancies associated with very poor prognosis. Although these cancers may initially respond to first-line treatment, they become highly resistant to standard chemotherapy in the metastatic setting. Chemotherapy resistance in basal-like breast cancers is associated with highly selective overexpression of the homeobox transcription factor *Engrailed 1* (*EN1*). Herein, we propose a novel therapeutic strategy using poly(glycidyl methacrylate) nanoparticles decorated with poly(acrylic acid) that enable dual delivery of docetaxel and interference peptides designed to block or inhibit EN1 (EN1-iPep). We demonstrate that EN1-iPep is highly selective in inducing apoptotic cell death in basal-like cancer cells with negligible effects in a non-neoplastic human mammary epithelial cell line. Furthermore, we show that treatment with EN1-iPep results in a highly synergistic pharmacological interaction with docetaxel in inhibiting cancer cell growth. The incorporation of these two agents in a single nanoformulation results in greater anticancer efficacy than current nanoparticle-based treatments used in the clinical setting.

Introduction

Triple negative breast cancers (TNBCs) are aggressive malignancies found in ~15% of all cases of breast cancer. Due to the lack of estrogen receptor, progesterone receptor, and human epidermal growth factor receptor-2 (HER-2) expression, TNBCs fail to respond to endocrine and anti-HER2 therapies.[1, 2] Currently, there are no approved targeted therapies against TNBCs and the treatment of choice is adjuvant chemotherapy using different compounds such as taxanes, platinum agents and PARP inhibitors.[3] The vast majority of TNBCs belong to the basal-like subtype, characterized by the presence of P53 and BRCA1 mutations.[4] While basal-like tumors initially respond to chemotherapy, in the metastatic setting they exhibit resistance and tumors relapse in most cases. Importantly, basal-like breast tumors aberrantly overexpress transcription factor Engrailed 1 (EN1. The functional role of EN1 has been extensively investigated in the context of the neural system, being expressed in dopaminergic neurons at early stages of embryonic development. Knockdown of EN1 by siRNA induces caspase-3 dependent dell death (apoptosis) in these neurons.[5] Additionally, EN1$^{+/-}$ mice show dopaminergic neuronal loss and degeneration[6], consistent with the neuronal phenotype of Parkinson-like disease.[7] In contrast, ectopic expression of EN1 promotes survival and protection against apoptosis in dopaminergic neurons. Alternatively, the presence of EN1 promotes survival and protection against apoptosis in dopaminergic neurons in the cerebellum.[6, 8] In the case of basal-like breast cancers, EN1 overexpression is associated with enhanced cell proliferation, metastasis, and increased drug resistance.[9] It has been demonstrated that knockdown of EN1 induces potent caspase-3 apoptosis and sensitizes basal-like breast cancer cells to chemotherapy.[9] This suggests that selectively inhibiting EN1 activity offers a novel route for the treatment of basal-like breast cancer. Transcription factors, unlike other molecular cancer targets such as tyrosine kinase receptors[10] have largely remained "undruggable" due to their small molecular binding pockets. However, we have previously reported interference peptides against EN1 (EN1-iPep) that overcome this problem.[9] EN1-iPep prevents transcription by binding to EN1 through a dominant negative-like mechanism, inhibiting interactions between EN1, its binding partners, and DNA. Currently, conventional chemotherapy is the mainstay of treatment for basal-like breast cancer. Of the various chemotherapeutics, docetaxel (DTX), a taxoid anticancer agent, is routinely used in the treatment of metastatic breast cancer.[11] Taxanes induce inhibition of cell proliferation in the S-phase through the promotion and stabilization of microtubule assembly, resulting in apoptosis.[12] The application of DTX and doxorubicin-loaded nanoparticles for TNBC treatment seems promising as they have previously been shown to exert greater antitumoral effects and reduced side effects than the free drugs both in vitro and in vivo.[13-17] These drugs exhibit a greater systemic circulatory half-life when applied in a nanoparticle form. However, mutations in BRCA1, which are a hallmark of patients with basal-like breast

[a] *Cancer Epigenetics, Harry Perkins Institute of Medical Research, Nedlands, WA 6009, Australia*
[b] *School of Chemistry & Biochemistry, The University of Western Australia, Crawley, WA 6009, Australia*

† These authors contributed equally to the work.
* Corresponding authors.
Email: pilar.blancafort@uwa.edu.au; swaminatha.iyer@uwa.edu.au
Electronic Supplementary Information (ESI) available: [details of any supplementary information available should be included here]. See DOI: 10.1039/x0xx00000x

cancer, are now proposed to be an important predictive factor in the development of resistance to docetaxel treatment.[18] The approaches used so far to chemosensitize tumors have relied on the development of alternative neoadjuvant, and adjuvant therapeutic regimes. These have met with limited success. In this work, we adopt a novel strategy to sensitize basal-like breast cancer to chemotherapy. Herein we use poly(acrylic acid)-decorated poly(glycidyl methacrylate) nanoparticles to encapsulate docetaxel and electrostatically assemble EN1-iPeps, to enable dual delivery in basal-like breast cancer. We demonstrate the efficacy of this approach in sensitizing basal-like breast cancers to chemotherapy. Using systematic assessment of individual therapeutic agents, we show high synergism using this combinatorial approach and superior anticancer efficacy compared to clinical nanoparticle-based treatments.

Results and discussion

In vitro toxicity assays in normal and basal-like breast cancer cells treated with EN1-iPeps

The EN1-iPeps are 22-residue peptides derived from the EN1 transcription factor with the following sequence: N-KKKRKVPLVWPAWVYCTRYSDR-C. This sequence corresponds to the active form of the peptide, which carries anti-cancer properties (EN1-iPepact). In the mutant (EN1-iPepmut) form, the two tryptophan residues at positions 10 and 13 were replaced by alanines (Figure 1A). The tryptophans are contained in a highly conserved hexamotif, WPAWVY, which is shared by the homeodomain superfamily of transcription factors. These two tryptophan residues are essential for the interaction between EN1 and their binding co-factors (PBX1 and HOX members) and DNA. Thus, the mutant form EN1-iPepmut was expected to bind poorly to EN1 and served as a negative control in the experiments. The N-terminus of the peptide carries a cell penetration/nuclear localisation sequence (CPP/NLS), KKKRV which is present in the Simian Virus 40 (SV40) large T antigen and is necessary for the internalization of the peptide through plasma and nuclear membranes[19]. The specificity and efficacy of the EN1-iPep in targeting basal-like breast cancer cells was first assessed using in vitro cell viability assays.

In order to determine if the EN1-iPep was selective for basal-like breast cancer cells, we performed viability assays using the CellTiter-Glo assay in the basal-like breast cancer cell lines T11 and SUM149 and in the normal breast epithelial cell line MCF10A after treating the cells with increasing concentrations of EN1-iPepact and EN1-iPepmut (0-50μM) for 24h. We observed that the EN1-iPepact induced cancer cell death in murine claudin-low T11 cells, derived from p53-/- transgenic mice, and in human basal-like SUM149 cells (Figure 1B-C) but not in the normal breast epithelial cell line MCF10A (Supporting Information, Figure S1). Having established the selectivity of EN1-iPepact for basal-like breast cancer cells, we next examined the mechanism by which EN1-iPepact induced cell death. We performed an immunofluorescence assay for the detection of cleaved caspase-3 (hallmark of apoptosis) in T11 and SUM149 cells after the treatment with 50μM of EN1-iPepact and EN1-iPepmut for 8h. In addition, a cell viability assay was done with the same conditions to assess the percentage of cell death induced by the treatments. Immunofluorescence and viability assays showed that 50 μM EN1-iPepact induced mainly caspase-3-dependent apoptosis in T11 or SUM149 cells after 8 h (Figure 1D-E). Cells treated with EN1-iPepact exhibited typical apoptotic features such as nuclei condensation, consistent with previous reports that EN1 and EN2 knockout mice show dopaminergic neuronal degeneration and apoptosis.[6,5,20] Of note, cells treated with the same concentration of EN1-iPepmut remained unaffected. Similarly, EN1 knockdown has no effect in normal cells that do not express the gene.[21]

Assessment of synergistic effects between docetaxel, doxorubicin and EN1-iPeps

Given that the overarching aim of this study is to sensititse TNBC to chemotherapy, it is a pivotal first step to examine the nature of the interaction between the EN1-iPepact and drugs. The interactions of two commonly used chemotherapeutic drugs for metastatic breast cancer treatment—doxorubicin and DTX—with EN1-iPep were measured using the median dose effect method in triple negative murine breast cancer cells (T11 cells).[22] The combination index (CI) derived using this method provides a valuable indication of the nature of interaction between two agents. To assess synergistic effects, T11 cells were treated with increasing concentrations of DTX alone (0-10μM), doxorubicin alone (0-25μM), EN1-iPepact alone (0-10μM) and the respective drug-iPep combinations for 24h. After the treatments, the cell viability and the fraction affected (mortality) were determined by CellTiter-Glo (Figure 2). The CI value, obtained with the Compusyn software, scored lower than 1 for all combinations of DTX and EN1-iPepact tested, indicating a synergistic interaction between these two agents. In contrast, the combination of doxorubicin and EN1-iPepact resulted in an antagonistic effect (CI > 1). Based on these results, DTX was selected for inclusion into the nanoparticle formulation.

Preparation and characterization of nanoparticles

The nanoparticle used in the current study consisted of a poly(glycidyl methacrylate) (PGMA) core. These nanoparticles were additionally functionalized with rhodamine B (RhB) for confocal imaging. The DTX-loaded PGMA nanoparticles were prepared using an oil in water emulsification process which yielded nanoparticles with a Z-average hydrodynamic diameter of 160.9 ± 0.8 nm (PDI: 0.08).[23] Nanoparticles had 3% (w/w) DTX drug loading determined using HPLC. PAA was covalently bound to the DTX-loaded PGMA nanoparticles to provide an anionic surface suitable for electrostatic conjugation with the positively charged EN1-iPep. The EN1-iPep sequence (and particularly the SV40 cellular internalization motif) is rich in positively-charge residues, facilitating electrostatic interactions with the anionic PAA. Binding efficiencies (by mass ratio) of the EN1-iPepact to PAA-PGMA (empty nanoparticles), PAA-PGMA-DTX (containing DTX in the particle core) and PAA-PGMA-RhB (containing, RhB) were 16.8 ± 2.5%, 20.1 ± 3.7% and 14.2 ± 1.7%, respectively, while the loading for EN1-iPepmut yielded 16.2 ± 1.6%, 23.6 ± 0.4% and 22.7 ± 1.8%, respectively. Incubation of EN1-iPep with the nanoparticles was monitored by a positive shift in the zeta potential (Figure S2) indicating successful attachment of the EN1-iPep on the nanoparticle

surface. Figure 3 shows a representation of the EN1-iPep nanoparticle containing DTX.

Internalisation and in vitro effects of EN1-iPep-docetaxel chimeric nanoparticles

To investigate the effect of EN1-iPep attachment on cellular association of our nanoparticles, T11 cells treated with nanoparticles bearing either EN1-iPepact, EN1-iPepmut, or no EN1-iPep ("blank") were examined by confocal microscopy. These nanoparticles were modified with the fluorescent dye rhodamine B to facilitate visualization. As shown in Figure 4A, nanoparticles bearing EN1-iPep associated efficiently with T11 cells. In contrast to the nanoparticles bearing EN1-iPepact, blank nanoparticles did not associate with cells. This could possibly be due to a negative zeta potential associated with blank nanoparticles. In accordance with these results, treatment of T11 cells with EN1-iPepact-decorated nanoparticles (but not EN1-iPepmut or blank nanoparticles) resulted in induction of 43% of apoptosis as assessed by the quantification of cleaved caspase 3 (CL-C3) positive cells after 8 h of treatment (Figure 4B).

We subsequently investigated if the combined treatment of EN1-iPep and DTX inhibited cell viability when these agents were assembled in PGMA nanoparticles. To test this, T11 cells were treated with increasing concentrations of PAA-PGMA nanoparticles for 24 and 48h (0 to 0.28 mg/mL). These nanoparticles were coated with an equivalent concentration of EN1-iPep (act or mut), (0 to 75μM). After the treatments, the percentage of cell survival was determined by CellTiter-Glo and the IC50 of formulations determined. (Figure 4C). The IC50 of nanoparticles bearing both EN1-iPepact and DTX was 0.23 mg mL^{-1} (13.9 μM EN1-iPep equivalent) after 24 h and 0.10 mg mL^{-1} (6.03 μM) after 48 h. The combination of DTX and EN1-iPepact was more potent than either component alone when delivered using nanoparticles. Nanoparticles bearing EN1-iPepmut did not reach 50% cell mortality at 24 or 48 h post-treatment regardless of DTX content. These results indicate that our formulations were successfully delivered into basal-like breast cancer cells and that the EN1-iPep on the nanoparticle surface enhanced the effects of DTX in inhibiting breast cancer cell growth. Similarly, other agents assembled in nanoparticles have been used in order to enhance the therapeutic potential of chemotherapeutic drugs such as antibodies, siRNAs or plasmid DNAs.[24-28] EN1 is only expressed in dopaminergic neurons and in certain malignancies such as neuroblastomas[29] and basal-like breast carcinomas[30,31] which are highly enriched in stem cell-like characteristics[32,30] but not in normal breast tissue. EN1 expression in basal-like breast cancers could explain their intrinsic multidrug resistance. In the same line as us, some researchers attempted to abrogate the stem cell phenotype using plasmidic cDNA or special nanocarriers which lead to the sensitization of glioblastoma and hepatic tumors to chemotherapeutic drugs such as temozolomide[28] and epirubicin.[33]

Anti-tumoral effect of EN1-iPep/DTX nanoparticles relative to clinically approved Abraxane®

Abraxane® consists of albumin-bound paclitaxel nanoparticles (130 nm in size) and was approved in 2005 for the treatment of metastatic breast cancer. Up to now, it is the only taxane nanoformulation approved by the FDA for the treatment of breast cancer. This nanoformulation has been proven to improve patients' response and delayed tumor progression in phase III trial.[17] Other paclitaxel nanoformulations are currently in phase II/III clinical trials, and one DTX PEGylated nanoparticle formulation, NKTR-105® is still in its phase I clinical trial. We investigated whether our nanoformulations were more efficient than Abraxane® in inducing cell death in basal-like breast cancer cell lines. To this aim, we performed viability assays by CellTiter-Glo in T11 cells treated for 24h and 48h with different concentrations of Abraxane® (0-0.28 mg/mL), the same concentrations of PAA-PGMA-DTX NPs and PAA-PGMA-DTX NPs coated with EN1-iPepact. The concentrations of EN1-iPep in the last NPs ranged from 0 to 20μM.. We observed that our DTX nanoparticles bearing EN1-iPepact were significantly more potent in comparison with Abraxane® at both time points when used at an equivalent nanoparticle concentration (Figure 5). Note that the paclitaxel loading in Abraxane® is superior to DTX loading in our DTX nanoparticles, 10% versus 3%. In the clinic, free DTX demonstrated to perform slightly better than free paclitaxel in metastatic breast cancer patients when used at 100mg m^{-2} and 175mg m^{-2} respectively. Taking this into account, we can conclude that our synthetized DTX nanoparticles are more potent than Abraxane®.[34] The finding that our DTX nanoparticles performed better than Abraxane® is of potential interest because of the improved potency in this study and the high specificity of EN1-iPep for basal-like breast cancers over non-basal breast cancer cell lines[9] and normal cells (Figure S1). These data further validate that EN1-iPep could be used to decrease the dose and potentially the off-target toxicity of current chemotherapeutic regimes.

In vivo anti-tumor activity of EN1-iPep-PAA-PGMA nanoparticles

To evaluate if nanoparticles bearing DTX and EN1-iPep inhibit tumor growth in vivo, we tested four different NPs formulations (Blank NPs coated with EN1-iPepmut, Blank NPs coated with EN1-iPepact, DTX NPs coated with EN1-iPepmut and DTX NPs coated with EN1-iPepact) in mice implanted with subcutaneous T11 tumor allografts. This model was derived from serial orthotopic transplantations of mammary tumors from a p53 null mouse into a p53 wild-type syngeneic recipient[32,30] and mimics human claudin-low tumors, the majority of which are triple negative. Additionally, the T11 model is highly enriched in transcription factors promoting proliferation, resembling the basal-like subtype of breast cancer, and these animals possess an intact immune system, which offers a more reliable interpretation of the tumor physiology. Tumor allografts were injected in the flank of BALB/c mice and were treated via intratumoral injection of nanoparticle solution in PBS (2.5 mg nanoparticles per injection) once tumors reached ~300 mm^3. A total of 5 injections were performed, every 2 days (blank arrows), (Figure 6A). Tumor sizes were determined by digital calliper. The animal group treated with DTX nanoparticles bearing EN1-iPepact showed a reduction in tumor growth at the end of the treatment phase and exhibited the highest survival relative to the other formulations (Figure 6B-C). In comparison, animals treated with formulations containing no DTX and bearing EN1-iPepmut were the first group to reach the endpoint. Interestingly, the growth of tumors treated with EN1-iPepact

nanoparticles was markedly inhibited between days 7 and 9 after the start of treatment and reached the endpoint of the experiment at day 14 ($p<0.03$).

DTX nanoparticles bearing EN1-iPep may inhibit tumor growth and extend survival in this model of breast cancer. These findings indicated a benefit with the co-administration of DTX and EN1-iPepact in the nanoparticle formulation, which delayed the progression and the recurrence of the tumors post-administration. This was supported by the histopathological analysis of the tumors, which demonstrated a significant increase (>50%) in apoptotic cells in the combinatorial treatment (iPepact and DTX) relative to single treatments (25%) ($p=0.002$ and 0.001 respectively), as assessed by terminal deoxynucleotidyl transferase (TdT)-mediated dUTP nick-end labelling (TUNEL) assay (Figure 6D). Haematoxylin/eosin staining of the tumor sections demonstrated increased tissue damage, and areas of intense necrosis, in tumors treated with nanoparticles delivering both EN1-iPepact and DTX over the other treatment groups, which correlated with the enhanced apoptosis in the double treatments. The significant increase in apoptotic nuclei in tumors treated with EN1-iPepact bearing DTX nanoparticles ($p=0.001$) is in agreement to the enhanced sensitivity to DTX observed when T11 cells were treated with EN1-iPepact (Figure 2) and with the delay in tumor recurrence and increased survival in mice (Figure 6).

Experimental

Materials and methods

Materials. All materials were purchased from Sigma-Aldrich unless stated otherwise. Docetaxel and doxorubicin were obtained from LC Laboratories, 97%, (Woburn; MA, USA). Glycidyl methacrylate (GMA, 97%) was passed through an alumina column to remove inhibitor prior to use, and stored at 4°C. 2,2'-azobis(2-methylpropionitrile) (AIBN, 0.2 M in toluene), methyl ethyl ketone (MEK; Fischer Chemical, ≥99%), Pluronic F-108 (Mn = 14,600 g mol^{-1}) and poly(acrylic acid sodium salt) (PAA, Mw = 5100 g mol^{-1}) were used as received. Active and mutant EN1-iPep were purchased from China Peptides, Ltd.

Methods

Synthesis, functionalization and characterization of nanoparticles. Poly(glycidyl methacrylate) (Mw = 454270, PDI = 1.79) was synthesized using a free-radical polymerization process. Glycidyl methacrylate was dissolved in MEK and using 2,2'-azobis(2-methylpropionitrile) as an initiator, the reaction was heated to reflux under an inert atmosphere. The mixture was allowed to cool and PGMA was precipitated in methanol and collected by filtration. PAA-PGMA-DTX nanoparticles were prepared according to a modified method as described previously.[35] 100 mg PGMA and 15 mg docetaxel was dissolved in a 1:3 mixture of chloroform and MEK (6 ml) was added dropwise into an aqueous solution of Pluronic F-108 (1.25% w/v, 30 ml) under vigorous stirring. No docetaxel was added for empty PAA-PGMA nanoparticles. The emulsion was homogenized with a probe-type ultrasonicator set at 4 WRMS for 1 min. Organic solvents were removed from the emulsion under reduced pressure. The solution was centrifuged at 3000 × g for 45 min to remove large aggregates and the supernatant was further centrifuged at 20,000 × g (15 mins) to isolate nanoparticles from excess surfactant. The nanoparticles were resuspended in 10 ml of PAA solution (100 mg ml^{-1}, pH 9.0), assisted by short periods of ultrasonication at 4 WRMS. The suspension was stirred at 70°C overnight to conjugate PAA to the PGMA nanoparticles. The resultant nanoparticles were centrifuged and resuspended in PBS immediately before use. EN1-iPeps, both active and mutant, were electrostatically attached to PGMA-PAA nanoparticles by incubation at room temperature in PBS (pH 8.0) overnight. Hydrodynamic size and zeta potential was measured using a Zetasizer Nano ZS (Malvern Instruments). In order to confirm the stability of PAA-PGMA-DTX and EN1-iPep-PAA-PGMA-DTX nanoparticles within physical environment, size, polydispersibility index (PdI) and zeta potential were determined in the nanoparticles with the presence of BSA, resuspended in PBS (Supplementary Figure 3A). For the chemical characterisation of the nanoparticles, we made use of Fourier transform infrared spectroscopy (FT-IR) in DTX-NPs. FT-IR of PGMA nanoparticles containing DTX shows a peak at 710 cm^{-1} characteristic of DTX (Supplementary Figure 3B).

Determination of docetaxel loading in nanoparticles. PAA-PGMA-DTX nanoparticles were lyophilized and weighed before being suspended in 1 ml of methanol. The suspension was vortexed regularly over 1 hr to assist in the dissolution of encapsulated docetaxel. The nanoparticles were removed via centrifugation (14,000 × g, 15 min) and the supernatant containing the dissolved free drug was analyzed using RP-HPLC. The measurements were performed on a Waters 2695 separation module with Waters 2489 UV/Vis detector (determination λ = 232 nm) using reverse phase isocratic elution (methanol:water, 70:30; 1.5 ml min^{-1}) through a C18 column (150 × 4.60 mm, 5 µm, 25 ± 5°C). The measurements were compared against a standard curve done in identical run conditions. Docetaxel loading in the PAA-PGMA-DTX nanoparticles was calculated with the following formula (Equation 1) and the mean ± SD values from three replicate determinations are reported.

(Equation 1)

$$\text{Docetaxel loading \% (w/w)} = \frac{\text{mass of docetaxel within nanoparticles}}{\text{mass of nanoparticles}} \times 100$$

Docetaxel release from the nanoparticles

Docetaxel release was quantified according to the method of Singh *et al*[36]. (p.351). Nanoparticles (1.00ml, 7.26 mg ml^{-1}) were placed in dialysis membrane (Mw cutoff 100 KDa) and dialysed against a sink solution (15ml) containing either PBS or PBS + 1% w/v Tween 80 in water bath at 37°C. Aliquots (10ml) were drawn from the sink solution at each time point, freeze dried, extracted with methanol (200µl), and quantified by HPLC (isocratic elution with 70:30

methanol/water; C18 column, 150x4.60 mm, 5µm, 25°C; retention time ~10 min). At each time point, 10ml fresh solution was added to the sink to maintain flux conditions (Supplementary Figure 3C).

Cell culture. The T11 cell line was derived from a murine basal-like breast tumor of a p53-/- Brca1-/- BALB/c mouse.[30, 32] SUM149 and MCF10A were purchased from Asterand (Detroit; MI, USA) and the American Type Culture Collection (Manassas; VA, USA), respectively. T11 and SUM149 were cultured in RPMI and DMEM-F/12 (Life Technologies; VIC, Australia) medium respectively. Both media were supplemented with 10% fetal bovine serum (Life Technologies) and 1% penicillin/streptomycin (Life Technologies). MCF10A were cultured in a DMEM-F/12 supplemented with 10% horse serum, 20 ng ml^{-1} EGF, 0.5 µg ml^{-1} hydrocortisone, 10 mg ml^{-1} insulin, 100 ng ml^{-1} cholera toxin and 1% penicillin/streptomycin (Life Technologies).

Cell viability and assessment of apoptosis. To assess the selective activity of EN1-iPeps, T11, SUM149 and MCF10A cells were treated with EN1-iPepact and EN1-iPepmut for 24 h at concentrations up to 50 µM. To assess the efficacy of EN1-iPep nanoparticles as compared to the commercial chemotherapeutic Abraxane® (paclitaxel-albumin nanoparticles), T11 cells were treated with different concentrations of uncoated DTX nanoparticles (without EN1-iPep; blank), EN1-iPepact-DTX nanoparticles and Abraxane® at up to 0.5 mg ml^{-1} of nanoparticles, equivalent to a range of EN1-iPep up to 36.3 µM, for 24 and 48 h. Cell viability for the aforementioned experiments was assessed using the CellTiter-Glo assay according to the manufacturer's protocol (Promega; NSW, Australia) and luminescence was measured using the EnVision 2012 Multilabel Reader (PerkinElmer; Waltham, MA, USA). IC50 of EN1-iPeps against the various cell types were calculated using the Graphpad Prism 6 statistical package. Apoptosis was assessed by means of immunofluorescence visualization of cleaved-caspase 3 positive cells. T11 and SUM149 cells were treated with active or mutant EN1-iPep at 50 µM for 8 h. Following treatments, cells were fixed with 4% paraformaldehyde for 20 minutes, washed twice with PBS, blocked with blocking solution (5% fetal bovine serum, 0.3% Triton X-100 in PBS) for 1 h, incubated with the anti-cleaved caspase 3 primary antibody (1:500 dilution; Cell Signaling Technology, QLD, Australia) in blocking solution overnight and further incubated with an anti-rabbit secondary Alexa Fluor 488-conjugated antibody (Cell Signaling Technology, QLD, Australia). Nuclei were stained with Hoechst 33258. The percentage of positive cleaved-caspase 3 cells was determined by counting green fluorescent cells versus total cells using a fluorescent microscope (Olympus IX71).

Assessment of drug combination effects. The combinatorial effect of doxorubicin and docetaxel with EN1-iPeps was assessed by the median effect method[22] proposed by Chou and Talalay, using the free Compusyn software. T11 cells were treated for 24 h with doxorubicin, docetaxel and EN1-iPepact in non-constant ratios at doses up to 25 µM, 10 µM and 10 µM respectively. Cell viability was assessed using CellTiter-Glo as mentioned previously. This method determines the combination index (CI) between two agents. Additive, antagonistic or synergistic interactions between two agents are indicated by CI = 1, > 1 or < 1 respectively.

Confocal imaging. T11 cells were grown on 12 mm diameter glass coverslips and treated with rhodamine B-conjugated blank, EN1-iPepact or EN1-iPepmut coated nanoparticles at 0.33 mg ml^{-1} in serum free media for 4 h. This concentration of nanoparticles corresponds to the amount of EN1-iPepact attached to the nanoparticles calculated experimentally to reach the IC50 (24 µM) when administered in T11 in a nanoparticle format. Cells were fixed with 4% paraformaldehyde and washed twice with PBS. Nuclei and actin filaments were stained with 5 µg ml^{-1} Hoechst 33258 and Alexa Fluor 488 phalloidin (Life Technologies) respectively for 20 min. Coverslips were mounted on slides using Slowfade mounting media (Life Technologies). Slides were visualized by confocal microscopy (Hoescht λ_{ex} = 397 nm, λ_{em} = 400-468 nm; Alexa Fluor 488 λ_{ex} = 488 nm, λ_{em} = 497-546 nm; rhodamine B λ_{ex} = 561 nm, λ_{em} = 579-676 nm; Leica TCS SP2).

Animal model and in vivo efficacy assessment of EN1-iPep nanoparticles. All animal experiments were performed in accordance with protocols approved by the Animal Ethics Committee of The University of Western Australia. To simulate an advanced model of basal-like breast cancer, T11 cells (2.5×10^4 cells) were resuspended in serum free media and BD Matrigel Matrix High Concentration (BD Bioscience, NSW, Australia) in a 1:1 ratio to a total volume of 100 µL and injected subcutaneously into the flanks of 5 week old BALB/cJ females (Animal Resources Centre, WA, Australia) using a 26G needle. Nine days after inoculation of cells, tumors reached an average volume of 279 mm^3. At this point, animals were randomly assigned to one of four different groups. All animals received a total of 5 intratumoral injections every two days containing 2.5 mg of nanoparticles coated with 0.5 mg EN1-iPep diluted in 100 µL of saline solution. The four treatments were: blank nanoparticles with EN1-iPepmut or EN1-iPepact, and docetaxel nanoparticles with EN1-iPepmut or EN1-iPepact. Width and length of tumors were measured every day using a digital caliper and tumor volumes were calculated using the modified ellipsoid formula; V = $Width^2$ x $\frac{1}{2}$ Length. Animals bearing tumors >800mm^3 were humanely sacrificed.

Immunohistochemical analysis of the tumors. Tumor tissues were fixed in 4% paraformaldehyde, washed 3 times in PBS and left in 70% ethanol. Tumors were embedded in paraffin and 5 µm sections were prepared. For haematoxylin/eosin staining, slides were dewaxed, hydrated using a decreasing solution bank of ethanol, stained with Gill's haematoxylin, dehydrated using 70% ethanol, stained with eosin, further dehydrated using 100% ethanol, cleared using toluene and mounted in coverslips using Acrymount IHC mounting media (McKinney, Texas, USA). Tumor cell apoptosis was determined

in tissue sections by TUNEL assay (In Situ Cell Death Detection Kit; Roche, VIC, Australia).

Statistical analysis. All in vitro experiments were performed in triplicate and repeated at least three times. Results were averaged and the standard deviation (SD) or standard error of the mean (SEM) was calculated as indicated in the figures. To determine statistical significance a two-tailed unpaired Student's t test was used between 2 different independent groups. * indicates $p<0.05$, ** indicates $p<0.005$ and *** indicates $p<0.0005$.

Conclusions

We demonstrate a novel approach to sensitize basal-like breast cancer to chemotherapy. The nanoparticles used in the current study enabled simultaneous administration of anticancer drug DTX and EN1-iPep, an inhibitor of the EN1 transcription factor that is overexpressed in basal-like triple negative breast cancer. We have shown that through this approach, EN1-iPep improves the potency of DTX compared to current commercial gold standard Abraxane® in reducing viability of stem cell-enriched T11 cells, and inhibits tumor growth and enhances survival in BALB/c mice implanted with T11 allografts. We believe these findings are highly significant in developing novel therapeutic strategies for the treatment of various cancers, particularly those that are currently classified undruggable.

Acknowledgements

A.S. holds a postdoctoral fellowship from the National Breast Cancer Foundation (PF-15-001). This research was supported by an Australian Research Council grants: DP150104433, FT130101688 and FT130101767, the Cancer Council of Western Australia Research Fellowship, National Health and Medical Research Council grant APP1069308, National Institutes of Health grants R01CA170370, R01DA036906, and the National Breast Cancer Foundation NC-14-024 to Pilar Blancafort. The authors acknowledge assistance from the Australian Microscopy & Microanalysis Research Facility at the Centre for Microscopy, Characterisation & Analysis, The University of Western Australia.

Notes and references

1. L. Carey, E. Winer, G. Viale, D. Cameron and L. Gianni, *Nature reviews. Clinical oncology*, 2010, **7**, 683-692.
2. C. M. Perou, T. Sorlie, M. B. Eisen, M. van de Rijn, S. S. Jeffrey, C. A. Rees, J. R. Pollack, D. T. Ross, H. Johnsen, L. A. Akslen, O. Fluge, A. Pergamenschikov, C. Williams, S. X. Zhu, P. E. Lonning, A. L. Borresen-Dale, P. O. Brown and D. Botstein, *Nature*, 2000, **406**, 747-752.
3. I. A. Mayer, V. G. Abramson, B. D. Lehmann and J. A. Pietenpol, *Clinical cancer research : an official journal of the American Association for Cancer Research*, 2014, **20**, 782-790.
4. C. M. Perou, *The oncologist*, 2010, **15 Suppl 5**, 39-48.
5. L. Alberi, P. Sgado and H. H. Simon, *Development*, 2004, **131**, 3229-3236.
6. D. Alvarez-Fischer, J. Fuchs, F. Castagner, O. Stettler, O. Massiani-Beaudoin, K. L. Moya, C. Bouillot, W. H. Oertel, A. Lombes, W. Faigle, R. L. Joshi, A. Hartmann and A. Prochiantz, *Nature neuroscience*, 2011, **14**, 1260-1266.
7. A. Hartmann, S. Hunot, P. P. Michel, M. P. Muriel, S. Vyas, B. A. Faucheux, A. Mouatt-Prigent, H. Turmel, A. Srinivasan, M. Ruberg, G. I. Evan, Y. Agid and E. C. Hirsch, *Proceedings of the National Academy of Sciences of the United States of America*, 2000, **97**, 2875-2880.
8. M. T. Alves dos Santos and M. P. Smidt, *Neural development*, 2011, **6**, 23.
9. A. S. Beltran, L. M. Graves and P. Blancafort, *Oncogene*, 2014, **33**, 4767-4777.
10. A. Sorolla, A. Yeramian, J. Valls, X. Dolcet, L. Bergada, A. Llombart-Cussac, R. M. Marti and X. Matias-Guiu, *Molecular oncology*, 2012, **6**, 530-541.
11. M. Martin, T. Pienkowski, J. Mackey, M. Pawlicki, J. P. Guastalla, C. Weaver, E. Tomiak, T. Al-Tweigeri, L. Chap, E. Juhos, R. Guevin, A. Howell, T. Fornander, J. Hainsworth, R. Coleman, J. Vinholes, M. Modiano, T. Pinter, S. C. Tang, B. Colwell, C. Prady, L. Provencher, D. Walde, A. Rodriguez-Lescure, J. Hugh, C. Loret, M. Rupin, S. Blitz, P. Jacobs, M. Murawsky, A. Riva, C. Vogel and I. Breast Cancer International Research Group, *The New England journal of medicine*, 2005, **352**, 2302-2313.
12. P. B. Schiff and S. B. Horwitz, *Proceedings of the National Academy of Sciences of the United States of America*, 1980, **77**, 1561-1565.
13. W. J. Gradishar, *Breast cancer : basic and clinical research*, 2012, **6**, 159-171.
14. J. Park, P. M. Fong, J. Lu, K. S. Russell, C. J. Booth, W. M. Saltzman and T. M. Fahmy, *Nanomedicine : nanotechnology, biology, and medicine*, 2009, **5**, 410-418.
15. G. Palma, C. Conte, A. Barbieri, S. Bimonte, A. Luciano, D. Rea, F. Ungaro, P. Tirino, F. Quaglia and C. Arra, *International journal of pharmaceutics*, 2014, **473**, 55-63.
16. M. Liang, K. Fan, M. Zhou, D. Duan, J. Zheng, D. Yang, J. Feng and X. Yan, *Proceedings of the National Academy of Sciences of the United States of America*, 2014, **111**, 14900-14905.
17. W. J. Gradishar, S. Tjulandin, N. Davidson, H. Shaw, N. Desai, P. Bhar, M. Hawkins and J. O'Shaughnessy, *Journal of clinical oncology : official journal of the American Society of Clinical Oncology*, 2005, **23**, 7794-7803.
18. M. Kriege, A. Jager, M. J. Hooning, E. Huijskens, J. Blom, C. H. van Deurzen, M. Bontenbal, J. M. Collee, M. B. Menke-Pluijmers, J. W. Martens and C. Seynaeve, *Cancer*, 2012, **118**, 899-907.
19. M. C. Morris, S. Deshayes, F. Heitz and G. Divita, *Biology of the cell / under the auspices of the European Cell Biology Organization*, 2008, **100**, 201-217.
20. P. Sgado, L. Alberi, D. Gherbassi, S. L. Galasso, G. M. Ramakers, K. N. Alavian, M. P. Smidt, R. H. Dyck and H. H. Simon, *Proceedings of the National Academy of Sciences of the United States of America*, 2006, **103**, 15242-15247.
21. A. S. Beltran, A. Russo, H. Lara, C. Fan, P. M. Lizardi and P. Blancafort, *PloS one*, 2011, **6**, e24595.

22. T. C. Chou and P. Talalay, *Advances in enzyme regulation*, 1984, **22**, 27-55.
23. C. W. Evans, M. Fitzgerald, T. D. Clemons, M. J. House, B. S. Padman, J. A. Shaw, M. Saunders, A. R. Harvey, B. Zdyrko, I. Luzinov, G. A. Silva, S. A. Dunlop and K. S. Iyer, *ACS nano*, 2011, **5**, 8640-8648.
24. J. Li, P. Cai, A. Shalviri, J. T. Henderson, C. He, W. D. Foltz, P. Prasad, P. M. Brodersen, Y. Chen, R. DaCosta, A. M. Rauth and X. Y. Wu, *ACS nano*, 2014, **8**, 9925-9940.
25. S. Su, Y. Tian, Y. Li, Y. Ding, T. Ji, M. Wu, Y. Wu and G. Nie, *ACS nano*, 2015, **9**, 1367-1378.
26. S. Inoue, R. Patil, J. Portilla-Arias, H. Ding, B. Konda, A. Espinoza, D. Mongayt, J. L. Markman, A. Elramsisy, H. W. Phillips, K. L. Black, E. Holler and J. Y. Ljubimova, *PloS one*, 2012, **7**, e31070.
27. W. Xu, T. Luo, P. Li, C. Zhou, D. Cui, B. Pang, Q. Ren and S. Fu, *International journal of nanomedicine*, 2012, **7**, 915-924.
28. S. S. Kim, A. Rait, E. Kim, K. F. Pirollo, M. Nishida, N. Farkas, J. A. Dagata and E. H. Chang, *ACS nano*, 2014, **8**, 5494-5514.
29. I. Ceballos-Picot, L. Mockel, M. C. Potier, L. Dauphinot, T. L. Shirley, R. Torero-Ibad, J. Fuchs and H. A. Jinnah, *Human molecular genetics*, 2009, **18**, 2317-2327.
30. A. Prat, J. S. Parker, O. Karginova, C. Fan, C. Livasy, J. I. Herschkowitz, X. He and C. M. Perou, *Breast cancer research : BCR*, 2010, **12**, R68.
31. Y. Su, A. Subedee, N. Bloushtain-Qimron, V. Savova, M. Krzystanek, L. Li, A. Marusyk, D. P. Tabassum, A. Zak, M. J. Flacker, M. Li, J. J. Lin, S. Sukumar, H. Suzuki, H. Long, Z. Szallasi, A. Gimelbrant, R. Maruyama and K. Polyak, *Cell reports*, 2015, **11**, 1549-1563.
32. P. J. Roberts, J. E. Usary, D. B. Darr, P. M. Dillon, A. D. Pfefferle, M. C. Whittle, J. S. Duncan, S. M. Johnson, A. J. Combest, J. Jin, W. C. Zamboni, G. L. Johnson, C. M. Perou and N. E. Sharpless, *Clinical cancer research : an official journal of the American Association for Cancer Research*, 2012, **18**, 5290-5303.
33. X. Wang, X. C. Low, W. Hou, L. N. Abdullah, T. B. Toh, M. Mohd Abdul Rashid, D. Ho and E. K. Chow, *ACS nano*, 2014, **8**, 12151-12166.
34. S. E. Jones, J. Erban, B. Overmoyer, G. T. Budd, L. Hutchins, E. Lower, L. Laufman, S. Sundaram, W. J. Urba, K. I. Pritchard, R. Mennel, D. Richards, S. Olsen, M. L. Meyers and P. M. Ravdin, *Journal of Clinical Oncology*, 2005, **23**, 5542-5551.
35. C. W. Evans, H. M. Viola, D. W. Ho, L. C. Hool, S. A. Dunlop, M. Fitzgerald and K. S. Iyer, *Rsc Adv*, 2012, **2**, 8587-8590.
36. R. Singh, M. Norret, M. J. House, Y. Galabura, M. Bradshaw, D. Ho, R. C. Woodward, T. G. Pierre, I. Luzinov, N. M. Smith, L. Y. Lim and K. S. Iyer, *Small*, 2016, **12**, 351-359.